J Pharmacol Sci **124**, 276 – 285 (2014)

*Journal of Pharmacological Sciences*


*Full Paper*

# Insulin Sensitization by a Novel Partial Peroxisome Proliferator-Activated Receptor γ Agonist With Protein Tyrosine Phosphatase 1B Inhibitory Activity in Experimental Osteoporotic Rats

Masahiro Kubo[1,2,*], Masaki Fukui[1], Yuma Ito[1], Tatsuya Kitao[1], Hiroaki Shirahase[1], Eiichi Hinoi[2], and Yukio Yoneda[2]

[1]*Research Laboratories, Kyoto Pharmaceutical Industries, Ltd., 38 Nishinokyo, Tsukinowa-cho, Nakagyo-ku, Kyoto 604-8444, Japan*
[2]*Laboratory of Molecular Pharmacology, Graduate School of Natural Science and Technology, Kanazawa University, Kanazawa, Ishikawa 920-1192, Japan*

*Received November 14, 2013; Accepted December 25, 2013*

**Abstract.** The pharmacological profile of (*S*)-7-(2-{2-[(*E*)-2-cyclopentylvinyl]-5-methyloxazol-4-yl}-ethoxy)-2-[(2*E*,4*E*)-hexadienoyl]-1,2,3,4-tetrahydroisoquinoline-3-carboxylic acid (KY-201), a peroxisome proliferator-activated receptor (PPAR) γ agonist, was compared with that of rosiglitazone in ovariectomized rats. The serum triglyceride and non-esterified fatty acid reducing effects of KY-201 at 3 and 10 mg/kg per day for 6 weeks were similar to those of rosiglitazone despite its weaker PPARγ agonistic activity. KY-201 had no effects on body weight gain, blood volume, or heart and adipose weights, while rosiglitazone at 10 mg/kg per day increased them. KY-201 had few effects on bone mineral density (BMD) or fat in marrow (FM), whereas rosiglitazone strongly decreased BMD and increased FM. The PPARγ agonistic activity of KY-201 was weaker than that of rosiglitazone in ST-2 cells, and KY-201 reduced osteoblast differentiation and increased adipocyte differentiation less potently than rosiglitazone in rat bone marrow-derived mesenchymal stem cells. KY-201, but not rosiglitazone inhibited protein tyrosine phosphatase 1B (PTP1B) and increased phosphorylation of the insulin receptor in HepG2 cells. These results suggest that the hypolipidemic effects of KY-201 are similar to those of rosiglitazone, but with less adverse effects, due to the combination of PPARγ partial activation and PTP1B inhibition. KY-201 would be useful for treatments of diabetic patients at high risk of osteoporosis, cardiovascular disease, and/or obesity.

***Keywords***: proliferator-activated receptor (PPAR) γ, protein tyrosine phosphatase 1B (PTP1B), diabetes, anti-hyperlipidemia, postmenopausal osteoporosis

## Introduction

The number of patients with type 2 diabetes has been increasing worldwide over the past few decades, and is now a serious global health burden. Type 2 diabetes causes hyperglycemia due to impaired insulin secretion and/or insulin resistance, resulting in glucotoxicity in various organs, which leads to severe complications including cardiovascular diseases, nephropathy, retinopathy, and peripheral neuropathy (1). Thus, patients with type 2 diabetes have been treated with insulin or insulin secretagogues such as sulfonylureas, glinides, dipeptidyl-peptidase IV (DPP-IV) inhibitors, and glucagon-like peptide-1 (GLP-1) analogues or insulin sensitizers such as metformin and glitazones to normalize hyperglycemia (2, 3). Although sulfonylureas and glinides effectively lower plasma glucose by stimulating insulin release from pancreatic beta cells, they may cause critical hypoglycemia (2). DPP-IV inhibitors and GLP-1 analogues stimulate insulin release in a glucose-dependent manner; therefore, they have been used as safer insulin-secretagogues (3, 4). Insulin sensitizers are effective

*Corresponding author. kubo@kyoto-pharm.co.jp
Published online in J-STAGE
doi: 10.1254/jphs.13236FP

in reducing plasma glucose without an increase in plasma insulin levels in type 2 diabetic patients with insulin resistance and hyperinsulinemia. However, only metformin and two glitazones are clinically used as insulin sensitizers. Metformin has been used for a long time, but has moderate efficacy and may cause lactic acidosis (5, 6). Although glitazones such as rosiglitazone and pioglitazone, peroxisome proliferator-activated receptor (PPAR) $\gamma$ agonists, have been used as effective insulin sensitizers, they have adverse effects such as fluid retention, hemodilution, body weight gain, hepatotoxicity, the risk of heart failure, and reductions in bone mineral density (BMD) (7, 8). Thus, a large number of PPAR$\gamma$ or PPAR$\alpha/\gamma$ agonists have been synthesized to find a safer and more efficacious insulin sensitizer; however, none have been successfully developed to date (9).

The novel PPAR$\alpha/\gamma$ agonist (*S*)-7-(2-{2-[(*E*)-2-cyclopentylvinyl]-5-methyloxazol-4-yl}-ethoxy)-2-[(2*E*,4*E*)-hexadienoyl]-1,2,3,4-tetrahydroisoquinoline-3-carboxylic acid (KY-201, Fig. 1) was reported to exhibit protein tyrosine phosphatase-1B (PTP1B) inhibitory activity (10). PTP1B is known as a non-receptor type tyrosine phosphatase and negatively regulates insulin and leptin signaling (11, 12). The genetic deletion or pharmacological intervention of PTP1B is known to have anti-diabetic and anti-obesity effects by amplifying insulin and leptin signaling, respectively (13, 14). KY-201 was previously reported to reduce plasma glucose and triglyceride (TG) levels more effectively than rosiglitazone in KK-A$^y$ mice, even though both compounds have similar human PPAR$\gamma$ agonistic activities in COS-1 cells (10), which suggests the involvement of PTP1B inhibition in its insulin-sensitizing effects. PPAR$\gamma$-related adverse effects such as fluid retention and hepatomegaly were weaker with KY-201 than with rosiglitazone in normoglycemic mice (10). However, its safety for cardiac hypertrophy, obesity, and reductions in BMD, all PPAR$\gamma$-related adverse effects, remains to be determined.

In the present study, the hypolipidemic effects and adverse effects of KY-201, including fluid retention, cardiac hypertrophy, obesity, and reductions in BMD, were compared with those of rosiglitazone, a PPAR$\gamma$ full agonist, in ovariectomized (OVX) female rats, which are used widely as an experimental osteoporosis model with normoglycemia, insulin resistance, mild obesity, and hyperlipidemia (15).

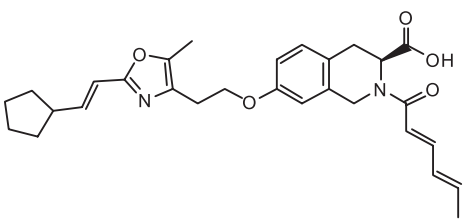


**Fig. 1.** Chemical structure of KY-201.

## Materials and Methods

*Materials and animals*

KY-201, rosiglitazone, and ertiprotafib were synthesized in our laboratories. ST-2 cells and HepG2 cells were purchased from Rikagaku Kenkyusho (Tsukuba) and Dainippon Sumitomo Pharma Co., Ltd. (Osaka), respectively. Roswell Park Memorial Institute (RPMI)-1640 medium and Dulbecco's modified Eagle's medium (DMEM, Nissui Pharmaceutical, Co., Ltd., Tokyo) or alpha Modified Eagle Minimum Essential Medium ($\alpha$-MEM; Life Technologies, Inc., Carlsbad, CA, USA) that contained 10% fetal bovine serum (JRH Bioscience, Inc., Lenexa, KS, USA), 0.3% $NaHCO_3$, and 1% penicillin-streptomycin were used for the cell culture. The anti-phosphorylated insulin receptor, anti-insulin receptor, and peroxidase-conjugated antibody were purchased from Merck Millipore (Billerica, MA, USA), Sntacruz (Dallas, TX, USA.) and Cell Signaling Technology, Inc. (Danvers, MA, USA), respectively. Female F344/NSlc rats were purchased from Japan SLC, Inc. (Hamamatsu) and individually housed under conditions with controlled temperature, humidity, and light exposure (12 h light–dark cycle) and were allowed ad libitum access to commercial standard rodent chow (CE-2; CLEA Japan, Inc., Tokyo) and tap water. Animals were handled in accordance with the "Guidelines for Animal Experimentation" approved by The Japanese Pharmacological Society, and all procedures were approved by the Animal Ethical Committee of Kyoto Pharmaceutical Industries. KY-201, rosiglitazone, and ertiprotafib were dissolved in dimethyl sulfoxide (DMSO; Nacalai Tesque, Kyoto); each drug solution was diluted in buffer or medium for in vitro study or suspended in 0.5% methylcellulose (Nacalai Tesque) for oral administration to animals.

*OVX rats and treatment*

Eight-week-old female F344/NSlc rats were anesthetized using ketamine (37.5 mg/kg, i.p.) and xylazine (7.5 mg/kg, i.p.), and bilateral ovariectomy was performed. Two days after surgery, OVX rats were randomized into 5 groups: vehicle-treated group and KY-201- and rosiglitazone-treated groups at 3 and 10 mg/kg per day. A sham-operated group and satellite group for a pharmacokinetic study were also used. Rats were orally administered vehicle or drugs for 6 weeks and then deeply

anaesthetized with pentobarbital sodium (50 mg/kg, i.p.). Blood was collected from abdominal aorta and total blood volumes were measured. Serum glucose, TG, and nonesterified fatty acid (NEFA) levels were measured colorimetrically using commercial kits (Wako Pure Chemical, Ind., Ltd.). Abdominal and subcutaneous adipose tissues, and hearts were isolated and weighed. Lumbar vertebra (L2 – L4) and bilateral femurs were fixed with 70% ethanol and stored at 4°C until the measurement of BMD. Lumbar vertebra and femurs were scanned by X-ray computed tomography (LaTheta; Aloka Co., Ltd., Tokyo) and reconstruct images were analyzed. After computed tomography analyses, the femurs were embedded in paraffin and 5-$\mu$m sections were cut on a rotary microtome. Sections were stained with hematoxylin and eosin. The relative area of fat in the marrow cavity was determined by microscopy (BZ-8100; Keyence Corporation, Osaka).

*Plasma concentrations of KY-201 and rosiglitazone*

Satellite groups of OVX rats were orally administered KY-201 and rosiglitazone at 3 and 10 mg/kg per day for 6 weeks. On day 42, blood samples were taken from the jugular vein at 0.25, 0.5, 1, 3, 5, 8, and 24 h after the drugs had been administered. Plasma concentrations of KY-201 and rosiglitazone were determined using a high performance liquid chromatography system consisting of a pump (PU-980; JASCO, Tokyo), UV detector (UV-970, JASCO), autoinjector (AS-950, JASCO), and Cosmosil-MS-II column (5 $\mu$m, 4.6 mm × 150 mm; Nacalai Tesque). The time to reach plasma maximal concentrations was between 0.5 and 1 h after the administration of KY-201 and rosiglitazone at doses of 3 and 10 mg/kg per day.

*PPAR$\gamma$ agonist activity*

ST-2 cells were cultured in RPMI1640 under 5% $CO_2$ at 37°C. The full-length mouse PPAR$\gamma$ 1 plasmid (Open Biosystems, Inc, Huntsville, AL, USA) and human RXR$\alpha$ plasmid (GeneCopoeia, Inc., Rockville, MD, USA) with the reporter plasmid pGL3-PPREx4-tk-luc were electroporated into ST-2 cells using Nucleofector II (AAD-1001S; Lonza, Basel, Switzerland). Cells were then seeded in 96-well plates at a density of $1.5 \times 10^3$ cells/well and incubated for 24 h in the presence or absence of the test compound. Luciferase activities were determined using a commercial kit (PicaGene LT7.5; TOYO B-Net CO., Ltd., Tokyo). Each maximal activity was taken as 100% and median effective concentration ($EC_{50}$) values were calculated.

*Isolation of rat bone marrow-derived mesenchymal stem cells (BMSCs)*

Bone marrow-derived mesenchymal stem cells were isolated from eight-week-old female F344/NSlc rats. Animals were deeply anesthetized with pentobarbital sodium (50 mg/kg, i.p.) and bled to death. The femoral bones were isolated and placed in fresh phosphate-buffered saline (PBS, pH 7.4) containing 1% penicillin–streptomycin. The bones were then cut at the ends and flushed with $\alpha$-MEM. After centrifugation, the precipitated cells were resuspended in $\alpha$-MEM and plated in 10-cm dishes at 5% $CO_2$ and 37°C. Adherent cells were then cultured for 1 week and used as BMSCs.

*In vitro osteoblast differentiation in rat BMSCs*

BMSCs were seeded in 96-well plates at a density of $4 \times 10^3$ cells/well. Test compounds were added 24 h later and cultured for 4 days. Cells were then washed with PBS (pH 7.4) and lysed in 50 $\mu$L saline containing 1% NP-40. The reaction was started by the addition of 50 $\mu$L of 10 mM *p*-nitrophenol phosphate in 50 mM ethanol amine and stopped by the addition of 50 $\mu$L of 1 N NaOH after 30 min incubation at 37°C. Alkaline phosphatase (ALP) activities were determined by measuring the absorbance at 405 nm.

*In vitro adipocyte differentiation*

BMSCs were seeded in 96-well plates at a density of $4 \times 10^3$ cells/well. Test compounds were added 24 h later and cultured for 4 days. Glycerol-3-phosphate dehydrogenase (GPDH) activities were measured using a commercial GPDH assay kit (Primary Cell Co., Ltd., Sapporo). BMSCs were seeded separately in 6-well plates at a density of $8 \times 10^4$ cells/well, and cultured for 4 days. Total RNA was prepared using Trizol (Life Technologies, Inc.) according to the manufacturer's instructions. PPAR$\gamma$2, CCAAT/enhancer-binding protein alpha (C/EBP$\alpha$), GPDH, lipoprotein lipase, adipocyte protein 2, and adiponectin mRNAs were determined by real-time polymerase chain reaction (real-time PCR).

*Real-time PCR*

To synthesize cDNAs, 0.1 $\mu$g total RNAs were reverse-transcribed using a commercial kit (Cosmo Bio Co., Ltd., Tokyo). The reaction was performed under the following conditions: synthesis at 37°C for 15 min and heat inactivation of reverse transcriptase at 85°C for 1 min. cDNAs were then stored at −30°C until use. Real-time PCRs were performed in 10 $\mu$L of the total reaction volume containing 5 $\mu$L of cDNAs, individual primer pairs, a fluorescently-labeled probe, and the commercial reagent (Light Cycler 480 Probes Master; Roche Diagnostics, Tokyo) according to the manufacturer's

protocol using Light Cycler 480 (Roche Diagnostics). Reactions were initiated by incubating at 95°C for 10 min and PCR (denaturation at 95°C for 10 s and annealing and extension at 60°C for 30 s) was performed for 45 cycles. The expression of each mRNA was standardized with 18S RNA. The sequences of primers were designed using the Universal ProbeLibrary (Roche Diagnostics): PPARγ2, 5′-GAAAGAAGCTGT GAACCACTAA-3′ and 5′-GAATGGCATCTCTGT GTCAA-3′; C/EBPα, 5′-ATAAAGCCAAACAGCGCA AC-3′ and 5′-CGGTCATTGTCACTGGTCAA-3′; GPDH, 5′-AGGGCCTCGTGGACAAGT-3′ and 5′-CAGGCA GCAGATGAACTCAC-3′; lipoprotein lipase, 5′-CAG AGAAGGGGCTTGGAGA-3′ and 5′-TTCATTCAG CAGGGAGTCAA-3′; adipocyte protein 2, 5′-GAG GAGACGAGATGGTGACAA-3′ and 5′-GCTCATGCC CTTTCGTAAAC-3′; adiponectin, 5′-TGGTCACAA TGGGATACCG-3′ and 5′-CCCTTAGGACCAAGA ACACCT-3′; 18S rRNA, 5′-GGTGCATGGCCGTTC TTA-3′ and 5′-TCGTTCGTTATCGGAATTAACC-3′.

*PTP1B inhibitory activity*

PTP1B inhibitory activities were determined in the absence or presence of the test compounds in 100 μL of 100 mM 4-(2-hydroxyethyl)-1-piperazineethanesulfonic acid (HEPES) buffer (pH 7.2) containing a human PTP1B enzyme (Enzo Life Sciences, Inc., Farmingdale, NY, USA), 3 mM *p*-nitrophenol phosphate, 1 mM dithiothreitol, 1 mM ethylenediaminetetraacetic acid (EDTA), and 0.001% Triton-X. The reaction was started by the addition of *p*-nitrophenol phosphate and stopped by the addition of 50 μL of 1N NaOH after 10 min incubation at 37°C, and absorbance was determined at 405 nm. The DMSO-treated enzymatic activity level was taken as 100%, and 50% inhibitory concentration ($IC_{50}$) was calculated.

*Insulin receptor phosphorylation in HepG2 cells*

HepG2 cells suspended in DMEM were seeded in 6-well plates at a density of $1 \times 10^6$ cells/well and cultured under 5% $CO_2$ at 37°C for 24 h and then for 6 h in serum-free DMEM. Cells were cultured in the presence or absence of test compounds for 1 h, followed by incubation with 1 nM insulin for 10 min. Cells were washed with 20 mM Tris-HCl buffer (pH 7.5) containing 5 mM EDTA-2Na, 10 mM sodium fluoride, 10 mM sodium β-glycerophosphate, 10 mM $Na_4P_2O_7$, and 10 mM $NaVO_4$; harvested; and suspended in 20 mM Tris-HCl buffer (pH 7.5) with 1 μg/mL *p*-amidinophenyl methanesulfonyl fluoride, leupeptin, 1 μg/mL antipain, 1 μg/mL benzamidine, and 1% Triton X-100. The suspensions were added at a volume of 4:1 to 50 mM tris(hydroxymethyl)aminomethane (Tris)-HCl buffer (pH 6.8) containing 10% sodium dodecylsulfate, 0.05% bromophenol blue, 50% glycerol, and 25% mercaptoethanol followed by heating and mixing at 100°C for 10 min. Each 30 μg aliquot of protein was loaded on a 7.5% polyacrylamide gel for electrophoresis at a constant current of 30 mA/plate for 1 h, followed by blotting to a polyvinylidene difluoride (PVDF) membrane previously treated with 100% methanol. After blocking by 10% skim milk dissolved in 20 mM Tris-HCl buffer (pH 7.5) containing 0.05% Tween 20 and 137 mM NaCl (TBS-T) for 1 h, the membrane was incubated with the anti-phosphorylated insulin receptor antibody or anti-insulin receptor monoclonal antibody diluted in TBS-T containing 1% skim milk (1:1000) followed by incubation with a peroxidase-conjugated antibody (1:1000). The protein content was determined using a chemiluminescence reagent (Chemi-Lumi One Super; Nacalai Tesque) and Chem Doc and Image Lab software (BioRad Laboratories, Inc., Hercules, CA, USA).

*Statistical analyses*

All data are expressed as the mean ± S.E.M. The significance of differences was assessed by a two-tailed student's *t*-test for paired data for in vitro assays and by Dunnett's multiple comparison test for in vivo assays.

## Results

*Effects of KY-201 and rosiglitazone in OVX rats*

The insulin sensitizing effects of KY-201 were previously shown to be 10 times stronger than those of rosiglitazone in KK-$A^y$ mice, despite its lower PPARγ activity and plasma concentration. In this study, hypolipidemic effects and adverse effects were investigated in OVX rats. Ovariectomy increased body weight gain, serum TG, and serum NEFA levels by 53%, 21%, and 22%, respectively, but had negligible effects on serum glucose levels. Rosiglitazone, but not KY-201 increased body weight gain at 10 mg/kg per day. KY-201 and rosiglitazone at 3 and 10 mg/kg per day reduced serum TG and NEFA levels to a similar extent (Table 1). Ovariectomy increased adipose tissue weight by 19%, but had negligible effects on heart weight and blood volume (Fig. 2). Rosiglitazone at 10 mg/kg per day significantly increased adipose tissue weight, heart weight, and blood volume, whereas KY-201 at both doses did not. The plasma maximal concentrations of KY-201 and rosiglitazone after their final administration were 0.54 and 6.17 μg/mL (1.1 and 12.5 μM, n = 2), respectively, at 3 mg/kg per day, and they were 3.56 and 17.99 μg/mL (10.0 and 50.3 μM, n = 2), respectively, at 10 mg/kg per day. Ovariectomy significantly decreased the BMDs of lumbar vertebra and femurs. Rosiglitazone

**Table 1.** Body weight gain and levels of serum glucose, TG, and NEFA in OVX rats treated with KY-201 and rosiglitazone

| | Sham operated | Control | KY-201 (mg/kg per day) | | Rosiglitazone (mg/kg per day) | |
|---|---|---|---|---|---|---|
| | | | 3 | 10 | 3 | 10 |
| Body weight gain (g) | 45.9 ± 2.4** | 70.4 ± 3.0 | 72.4 ± 3.4 | 72.4 ± 3.4 | 71.6 ± 3.8 | 82.8 ± 2.1* |
| Glucose (mg/dL) | 146 ± 9 | 153 ± 4 | 163 ± 8 | 146 ± 4 | 150 ± 3 | 152 ± 7 |
| TG (mg/dL) | 38 ± 6 | 46 ± 10 | 28 ± 5 | 25 ± 4 | 28 ± 4 | 25 ± 2 |
| NEFA (mEq/L) | 0.50 ± 0.02 | 0.61 ± 0.03 | 0.54 ± 0.03 | 0.43 ± 0.02** | 0.48 ± 0.02* | 0.41 ± 0.02** |

The values are the mean ± S.E.M. (n = 8). *$P$ < 0.05 and **$P$ < 0.01 vs. the Control group.

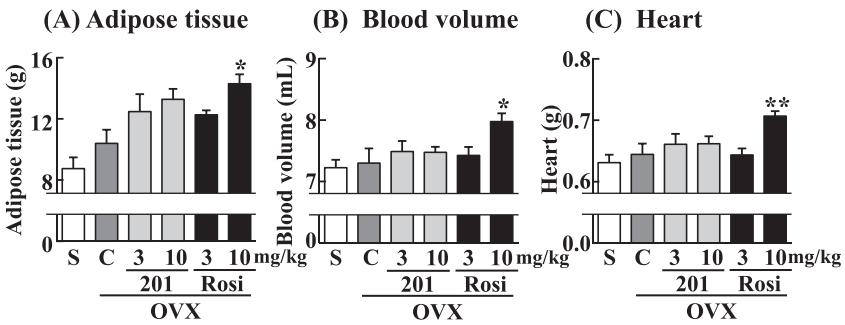


**Fig. 2.** Adipose tissue weight, blood volume, and heart weight in OVX rats treated with KY-201 and rosiglitazone for 6 weeks. The values are the mean ± S.E.M. (n = 8). S, Sham-operated; C, Control; 201, KY-201; Rosi, rosiglitazone. *$P$ < 0.05 and **$P$ < 0.01 vs. the Control group.

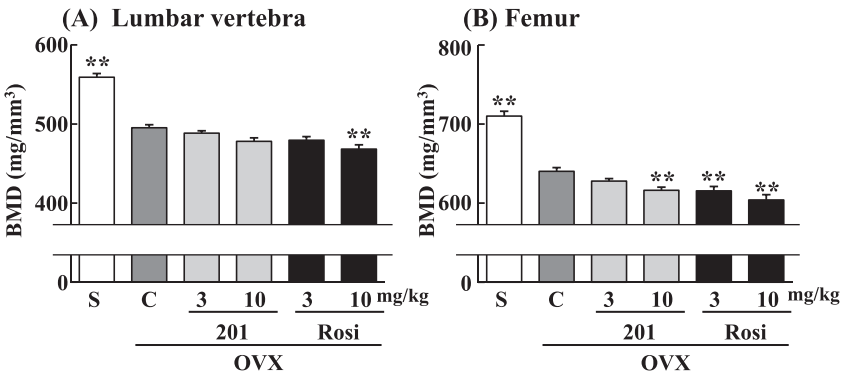


**Fig. 3.** Bone mineral density of lumbar vertebra and femur in OVX rats treated with KY-201 and rosiglitazone for 6 weeks. The values are the mean ± S.E.M. (n = 8). S, Sham-operated; C, Control; 201, KY-201; Rosi, rosiglitazone. *$P$ < 0.05 and **$P$ < 0.01 vs. the Control group.

significantly decreased the BMD of lumbar vertebra at 10 mg/kg per day, while KY-201 did not (Fig. 3A). KY-201 at 10 mg/kg per day and rosiglitazone at both 3 and 10 mg/kg per day significantly decreased the BMD of the femur (Fig. 3B). On hematoxylin and eosin staining analysis of sections, rosiglitazone more apparently increased fat in bone marrow cavity than KY-201 in femurs (Fig. 4A). Ovariectomy increased fat in the marrow cavity by 10%. Rosiglitazone further increased fat in the marrow cavity by 17% at 3 mg/kg per day and significantly increased it by 27% at 10 mg/kg per day, whereas KY-201 had no effect (Fig. 4B).

*PPARγ agonist activities*

The transactivation of PPAR$\gamma$ was investigated using a luciferase reporter assay. KY-201 and rosiglitazone at $10^{-7}$ – $10^{-5}$ M activated mouse PPAR$\gamma$ in a concentration-dependent manner. KY-201 was 2 times weaker than rosiglitazone ($EC_{50}$: 287 ± 88 and 148 ± 39 nM, respectively). The maximal activation level by KY-201 was 54.1% ± 1.1% that of rosiglitazone (Fig. 5).

*Effects on osteoblast and adipocyte differentiation in BMSCs*

In rat BMSCs, rosiglitazone significantly decreased ALP activities from $10^{-9}$ M in a concentration-dependent manner, while KY-201 significantly decreased it from $10^{-7}$ M. The reducing effects of KY-201 were significantly weaker than those of rosiglitazone at $10^{-8}$ – $10^{-5}$ M (Fig. 6A). KY-201 and rosiglitazone significantly increased GPDH activities from $10^{-7}$ M in a concentration-dependent manner, although the effects of KY-201

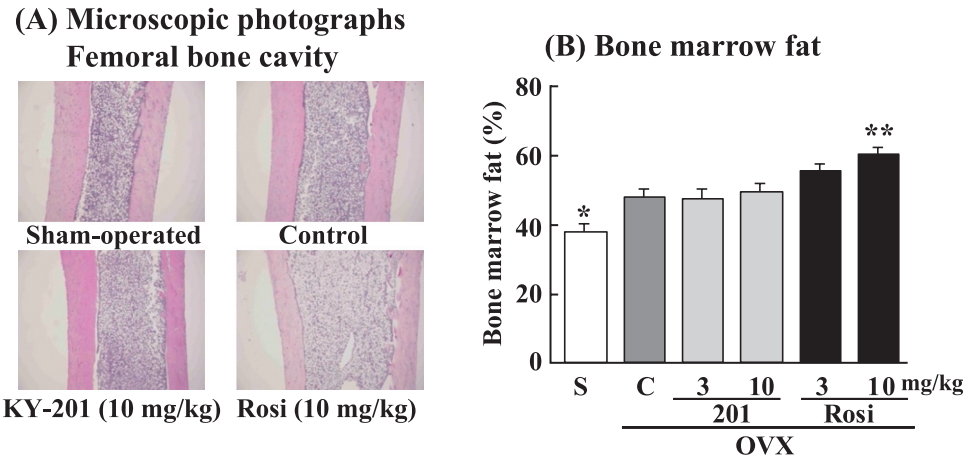


**Fig. 4.** Representative microscopic photographs of bone marrow cavities and the relative area of fat in the marrow cavity in OVX rats treated with KY-201 and rosiglitazone for 6 weeks. The values are the mean ± S.E.M. (n = 8). Fat (White area) in bone marrow cavities was measured in arbitrary 0.25 $mm^2$ area of femoral diaphyses. S, Sham-operated; C, Control; 201, KY-201; Rosi, rosiglitazone. $^{*}P < 0.05$ and $^{**}P < 0.01$ vs. the Control group.

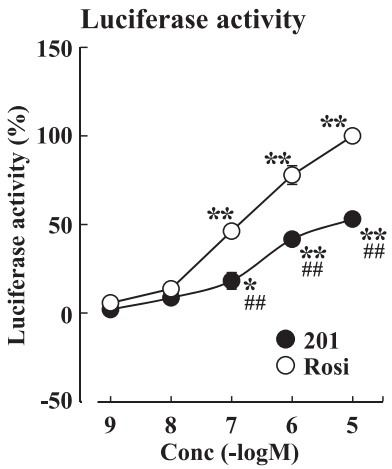


**Fig. 5.** Transactivation of mouse PPARγ by KY-201 and rosiglitazone in ST-2 cells. The activation level in rosiglitazone ($10^{-5}$ M)-treated cells was taken as 100% and that in the DMSO-treated cells was taken as 0%. The values are the mean ± S.E.M. (n = 3). $^{*}P < 0.05$ and $^{**}P < 0.01$ vs. DMSO-treated cells. 201, KY-201; Rosi, rosiglitazone. $^{\#}P < 0.05$ and $^{\#\#}P < 0.01$ vs. rosiglitazone-treated cells.

were significantly weaker than those of rosiglitazone at $10^{-6}$ M and $10^{-5}$ M (Fig. 6B).

*Effects on adiponenic gene expression in BMSCs*

The effects of KY-201 and rosiglitazone on adipocyte marker genes expression were examined in BMSCs. KY-201 and rosiglitazone increased the expression levels of genes involved in adipocyte differentiation: PPARγ, cEBPα, GPDH, lipoprotein lipase, adipocyte protein 2, and adiponectin, in a concentration-dependent manner. Although the effects of both drugs were similar at $10^{-9}$ – $10^{-7}$ M, the effects of KY-201 at higher than $10^{-7}$ M were weaker than that of rosiglitazone; increases in expression levels by KY-201 at $10^{-6}$ and $10^{-5}$ M were approximately 30% – 80 % those of rosiglitazone (Fig. 7).

*Effects on PTP1B activity and insulin receptor phosphorylation*

KY-201 and ertiprotafib, a PTP1B inhibitor (16), inhibited PTP1B activity in a concentration-dependent manner, whereas rosiglitazone did not. The $IC_{50}$ values of KY-201 and ertiprotafib were 3.7 ± 1.0 and 0.64 ± 0.24 μM, respectively (Fig. 8A). The insulin sensitizing effect of KY-201 was examined in a cell-based phos-

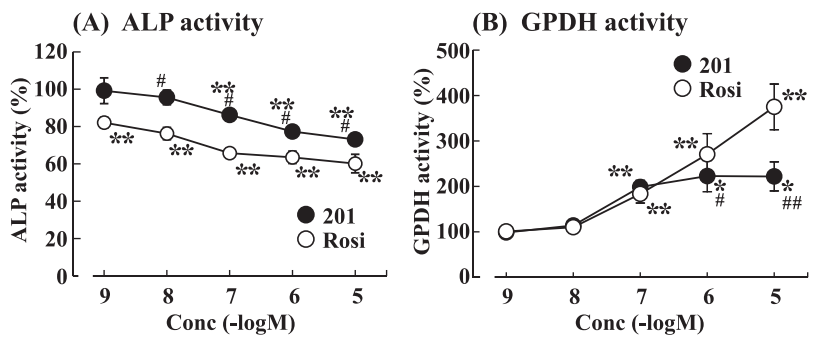


**Fig. 6.** ALP and GPDH activities in rat primary bone marrow cells cultured with KY-201 or rosiglitazone. ALP and GPDH activity levels in DMSO-treated cells were taken as 100% (120 ± 12 and 0.52 ± 0.07 unit, respectively). The values are the mean ± S.E.M. (n = 5). 201, KY-201; Rosi, rosiglitazone. $^{*}P < 0.05$ and $^{**}P < 0.01$ vs. DMSO-treated cells. $^{\#}P < 0.05$ and $^{\#\#}P < 0.01$ vs. rosiglitazone-treated cells.

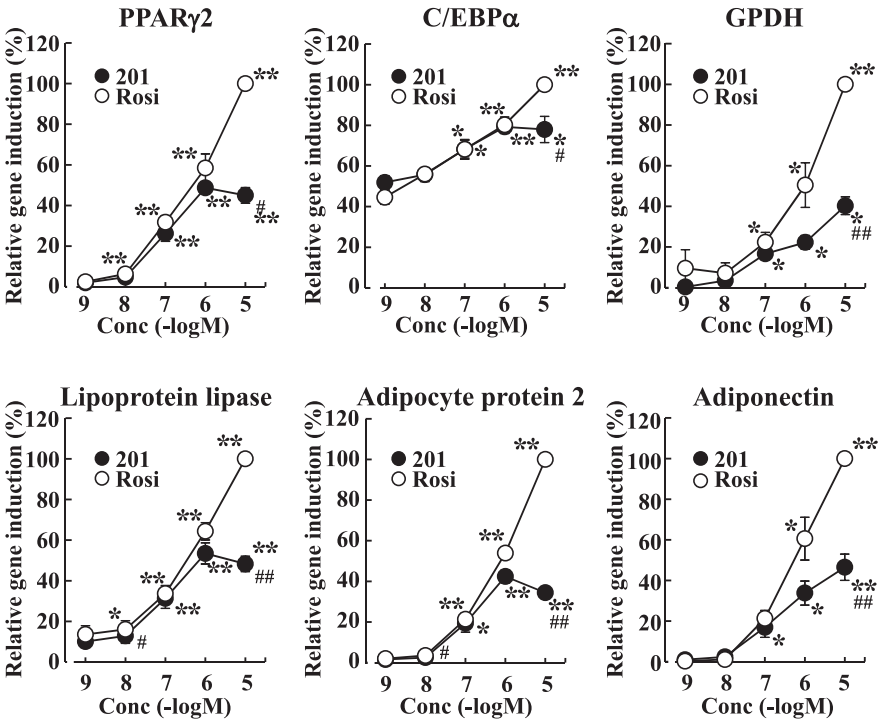


**Fig. 7.** Gene expression in rat primary bone marrow cells treated with KY-201 or rosiglitazone. The expression level induced by $10^{-5}$ M rosiglitazone was taken as 100%. The values are the mean ± S.E.M. (n = 4). 201, KY-201; Rosi, rosiglitazone. $^{*}P < 0.05$ and $^{**}P < 0.01$ vs. DMSO-treated cells. $^{\#}P < 0.05$ and $^{\#\#}P < 0.01$ vs. rosiglitazone-treated cells.

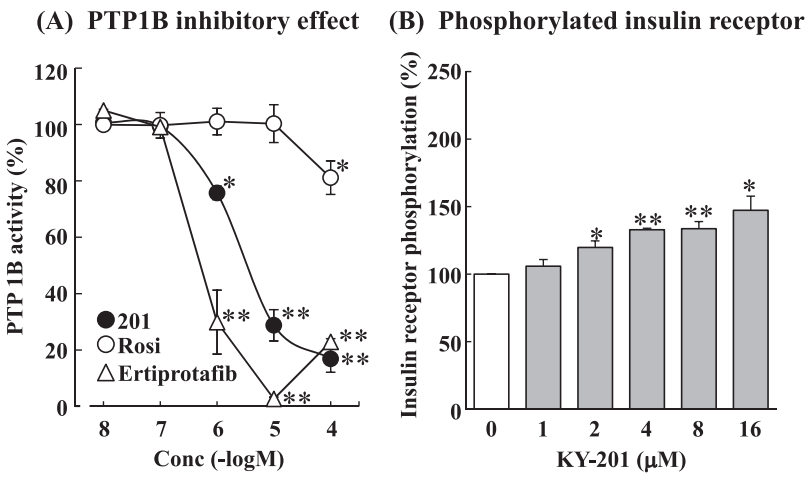


**Fig. 8.** PTP1B enzyme activity treated with KY-201, rosiglitazone and ertiprotafib (A) and phosphorylation of insulin receptor induced by insulin in KY-201-treated HepG2 cells (B). A: The DMSO-treated enzymatic activity level was taken as 100%, and the values are the mean ± S.E.M. (n = 3). 201; KY-201, Rosi; rosiglitazone. $^{*}P < 0.05$ and $^{**}P < 0.01$ vs. DMSO-treated. B: The phosphorylation level in DMSO-treated cells was taken as 100%, and the values are the mean ± S.E.M. (n = 4). $^{*}P < 0.05$ and $^{**}P < 0.01$ vs. DMSO-treated cells.

phorylation assay. KY-201 significantly potentiated insulin-induced insulin receptor phosphorylation from $2 \times 10^{-6}$ M in a concentration-dependent manner (Fig. 8B).

## Discussion

The present study was undertaken to determine whether KY-201 showed hypolipidemic effects with less adverse effects than rosiglitazone in OVX rats, and, if any, to clarify their mechanisms. OVX rats are an experimental model for osteoporosis in postmenopausal woman, which shows a marked reduction in BMD, obesity, and hyperlipidemia, but not hyperglycemia (15, 17). TG and NEFA, but not glucose levels were slightly increased by ovariectomy, and these increased TG and NEFA levels were similarly reduced by KY-201 and rosiglitazone. Insulin is known to lower plasma TG and NEFA levels by inhibiting very-low-density lipoprotein (VLDL) secretion from hepatocytes and uptake into adipocytes via lipoprotein lipase activation (18, 19). PPAR$\gamma$ agonists have been shown to reduce TG and NEFA levels by insulin sensitization in diabetic rats (20). However, KY-201 was found to exhibit partial human PPAR$\gamma$ agonistic activity in COS-1 cells (10),

and its plasma concentrations in OVX rats were approximately 10 times lower than those of rosiglitazone. Thus, the effects of KY-201 appear to be attributed, at least in part, to activity other than PPARγ agonistic activity. KY-201, but not rosiglitazone, inhibited PTP1B and increased insulin-stimulated insulin receptor phosphorylation in HepG2 cells. PTP1B is known to negatively regulate the insulin signal by dephosphorylating the insulin receptor and insulin receptor substrate phosphorylated by insulin (11). The overexpression of PTP1B in muscle has been proposed to cause insulin resistance (21). Hepatic deletion and PTP1B inhibitors were shown to improve insulin resistance and reduce plasma glucose and TG levels in diabetic mice (14, 22). The plasma concentrations of KY-201 in OVX rats were compatible with PTP1B inhibitory concentrations. It is likely that KY-201 showed hypolipidemic effects by partial PPARγ activation and PTP1B inhibition, the effects of which were similar to those of rosiglitazone by full PPARγ activation. Similar phenomena were observed in normoglycemic Zucker fatty rats with insulin resistance. KY-201 and rosiglitazone showed similar reducing effects on TG and NEFA levels and on elevated glucose levels in a glucose tolerance test (unpublished data). On the other hand, PTP1B inhibition was considered to more effectively exert insulin-sensitizing effects in diabetic mice; the hypoglycemic and hypolipidemic effects of KY-201 were approximately 10 times stronger than those of rosiglitazone, although its PPARγ activation levels and plasma concentrations were lower (10). However, the reason why the plasma maximal concentration of KY-201 was lower than that of rosiglitazone is not clarified so far. Differences in molecular weights and/or acidic moieties could affect the plasma maximal concentrations.

Only a high dose of rosiglitazone significantly increased body weight gain, adipose tissue weight, blood volume, and heart weight in OVX rats, which are all considered to be PPARγ-mediated adverse effects. PPARγ agonists promote adipocyte differentiation from preadipocytes in abdominal and subcutaneous adipose tissue, resulting in adiposity (23). PPARγ agonist–induced fluid retention is attributed to the activation of epithelial $Na^+$ channel subunit gamma in the collecting duct and/or to $Na^+$, $K^+$ATPase activation via proximal tubular PPARγ (24). The cardiac hypertrophy caused by PPARγ agonists appears to be induced by increased cardiac preload through fluid retention and/or cardiomyotic PPARγ activation (25, 26). The increase in body weight gain may be due to adiposity and/or fluid retention. CT analyses demonstrated that ovariectomy reduced BMD in lumbar vertebra and femurs. BMDs in these regions were markedly lower due to the rosiglitazone treatment than the KY-201 treatment. Insulin promotes osteoblastogenesis (27) and type 2 diabetic patients are at higher risk of bone fractures (8). PPARγ agonists are more likely to increase the risk of bone fractures in diabetic patients. Rosiglitazone and pioglitazone have been reported to increase the risk of bone fracture by decreasing BMDs in aged women (2, 8), which is explained by a shift from osteoblast differentiation to adipocyte differentiation by PPARγ activation in BMSCs (28, 29). Rosiglitazone, but not KY-201 markedly increased fat in the bone marrow cavity in OVX rats.

KY-201 has weaker adverse effects than rosiglitazone and this is considered to be due to its weaker PPARγ agonistic activity. The PPARγ agonistic activity of KY-201, which was reported using human PPARγ in COS-1 cells (10), was re-examined with a transactivation assay using murine PPARγ in ST-2 cells because transactivation activity varies depending on gene and cell types. The affinity and maximal activation levels of KY-201 were 2 times lower than those of rosiglitazone. ST-2 cells can differentiate into osteoblasts and adipocytes (30, 31), and PPARγ agonists are known to promote adipocyte differentiation, resulting in a reduction in osteoblast differentiation (28, 29). The weak PPARγ partial agonistic activity of KY-201 suggests that KY-201 more weakly promotes adipocyte differentiation and reduces osteoblast differentiation than rosiglitazone in mesenchymal stem cells. In rat BMSCs, rosiglitazone markedly increased GPDH activity, an adipocyte marker enzyme, and reduced ALP activity, an osteoblast marker enzyme; however, the effects of KY-201 at higher concentrations were significantly weaker than those of rosiglitazone. The increasing effects of KY-201 on the expression of PPARγ2, C/EBPα, GPDH, lipoprotein lipase, adipocyte protein 2, and adiponectin, all biomarker genes of adipocytes (29, 32), were also weaker than those of rosiglitazone in rat BMSCs cells. These findings demonstrate that KY-201 partially activates PPARγ, unlike rosiglitazone, a full PPARγ agonist, resulting in fewer PPARγ-mediated adverse effects.

KY-201 activates human, but not rodent PPARα (ref. 10 and unpublished data), leading to hypocholesterolemic and body weight reducing effects in patients. PPARα agonists are known to have cholesterol- and TG-reducing effects, improve insulin sensitivity, and may also reduce body weight (33, 34). KY-201 increased hepatic Acy-CoA activities in hamsters and reduced plasma cholesterol levels in hamsters, beagles, and monkeys (ref. 10 and unpublished data). The multifaceted characteristics of KY-201, including weak PPARγ and PPARα agonistic activities and PTP1B inhibitory activities, may beneficially exert additive and/or syner-

gistic effects in the treatment of type 2 diabetic patients at risk of cardiovascular disease, osteoporosis, and obesity. The therapeutic potentiality of KY-201 could be further clarified in future studies using diabetic OVX rats or diabetic hamsters.

In conclusion, KY-201, a partial PPAR$\alpha/\gamma$ agonist with PTP1B inhibitory activities, exhibits TG- and NEFA-reducing effects via insulin sensitization by the combination of PTP1B inhibitory activity and partial PPAR$\gamma$ agonistic activity; and it has fewer PPAR$\gamma$-mediated adverse effects such as reductions in BMD as well as fluid retention, cardiac hypertrophy, and increases in body and adipose weights due to partial PPAR$\gamma$ activation. The combination of partial PPAR$\gamma$ agonistic activities and PTP1B inhibitory activities is suggested to be a useful and effective approach in the treatment of type 2 diabetic patients at high risk of osteoporosis as well as cardiovascular disease and obesity.

## Conflicts of Interest

M.K., M.F., Y.I., T.K., and H.S. are employees of Kyoto Pharmaceutical Industries; E.H. and Y.Y. have no conflicts of interest.

## References


1 Deshpande AD, Harris-Hayes M, Schootman M. Epidemiology of diabetes and diabetes-related complications. Phys Ther. 2008; 88:1254–1264.

2 Kahn SE, Haffner SM, Heise MA, Herman WH, Holman RR, Jones NP, et al. Glycemic durability of rosiglitazone, metformin, or glyburide monotherapy. N Engl J Med. 2006;355:2427–2443.

3 Chia CW, Egan JM. Incretin-based therapies in type 2 diabetes mellitus. J Clin Endocrinol Metab. 2008;93:703–716.

4 Schnabel CA, Wintle M, Kolterman O. Metabolic effects of the incretin mimetic exenatide in the treatment of type 2 diabetes. Vasc Health Risk Manag. 2006;2:69–77.

5 Stang M, Wysowski DK, Butler-Jones D. Incidence of lactic acidosis in metformin users. Diabetes Care. 1999;22:925–927.

6 Renda F, Mura P, Finco G, Ferrazin F, Pani L, Landoni G. Metformin-associated lactic acidosis requiring hospitalization. A national 10 year survey and a systematic literature review. Eur Rev Med Pharmacol Sci. 2013;Suppl 1:45–49.

7 Krische D. The glitazones: proceed with caution. West J Med. 2000;173:54–57.

8 Lecka-Czernik B. Bone loss in diabetes: use of antidiabetic thiazolidinediones and secondary osteoporosis. Curr Osteoporos Rep. 2010;8:178–184.

9 Cho N, Momose Y. Peroxisome proliferator-activated receptor gamma agonists as insulin sensitizers: from the discovery to recent progress. Curr Top Med Chem. 2008;8:1483–1507.

10 Otake K, Azukizawa S, Fukui M, Shibabayashi M, Kamemoto H, Miike T, et al. A novel series of (S)-2,7-substituted-1,2,3,4-tetrahydroisoquinoline-3-carboxylic acids: peroxisome proliferator-activated receptor $\alpha/\gamma$ dual agonists with protein-tyrosine phosphatase 1B inhibitory activity. Chem Pharm Bull. 2011;59: 1233–1242.

11 Cheng A, Dubé N, Gu F, Tremblay ML. Coordinated action of protein tyrosine phosphatases in insulin signal transduction. Eur J Biochem. 2002;269:1050–1059.

12 Lund IK, Hansen JA, Andersen HS, Møller NP, Billestrup N. Mechanism of protein tyrosine phosphatase 1B-mediated inhibition of leptin signalling. J Mol Endocrinol. 2005;34: 339–351.

13 Picardi PK, Calegari VC, Prada PO, Moraes JC, Araújo E, Marcondes MC, et al. Reduction of hypothalamic protein tyrosine phosphatase improves insulin and leptin resistance in diet-induced obese rats. Endocrinology. 2008;149:3870–3880.

14 Fukuda S, Ohta T, Sakata S, Morinaga H, Ito M, Nakagawa Y, et al. Pharmacological profiles of a novel protein tyrosine phosphatase 1B inhibitor, JTT-551. Diabetes Obes Metab. 2010; 12:299–306.

15 Ma B, Zhang Q, Wang GJ, A JY, Wu D, Liu Y, et al. GC-TOF/MS-based metabolomic profiling of estrogen deficiency-induced obesity in ovariectomized rats. Acta Pharmacol Sin. 2011;32:270–278.

16 Shrestha S, Bhattarai BR, Cho H, Choi JK, Cho H. PTP1B inhibitor Ertiprotafib is also a potent inhibitor of IkappaB kinase beta (IKK-beta). Bioorg Med Chem Lett. 2007;17:2728–2730.

17 Li M, Healy DR, Li Y, Simmons HA, Gao F, Ke HZ, et al. A comparison of the anabolic effects of rat and bovine parathyroid hormone (1-34) in ovariectomized rats. J Musculoskelet Neuronal Interact. 2001;2:77–83.

18 Malmström R, Packard CJ, Caslake M, Bedford D, Stewart P, Yki-Järvinen H, et al. Defective regulation of triglyceride metabolism by insulin in the liver in NIDDM. Diabetologia. 1997;40:454–462.

19 Goldberg IJ, Eckel RH, Abumrad NA. Regulation of fatty acid uptake into tissues: lipoprotein lipase- and CD36-mediated pathways. J Lipid Res. 2009;50:S86–S90.

20 Yang B, Brown KK, Chen L, Carrick KM, Clifton LG, McNulty JA, et al. Serum adiponectin as a biomarker for in vivo PPARgamma activation and PPARgamma agonist-induced efficacy on insulin sensitization/lipid lowering in rats. BMC Pharmacol. 2004;4:1–9.

21 Zabolotny JM, Haj FG, Kim YB, Kim HJ, Shulman GI, Kim JK, et al. Transgenic overexpression of protein-tyrosine phosphatase 1B in muscle causes insulin resistance, but overexpression with leukocyte antigen-related phosphatase does not additively impair insulin action. J Biol Chem. 2004;279:24844–24851.

22 Haj FG, Zabolotny JM, Kim YB, Kahn BB, Neel BG. Liver-specific protein-tyrosine phosphatase 1B (PTP1B) re-expression alters glucose homeostasis of PTP1B-/-mice. J Biol Chem. 2005;280:15038–15046.

23 Rosen ED, Sarraf P, Troy AE, Bradwin G, Moore K, Milstone DS. PPAR gamma is required for the differentiation of adipose tissue in vivo and in vitro et al. Mol Cell. 1999;4:611–617.

24 Bełtowski J, Rachańczyk J, Włodarczyk M. Thiazolidinedione-induced fluid retention: recent insights into the molecular mechanisms. PPAR Res. 2013;2013:1–8.

25 Hasegawa H, Takano H, Komuro I. Therapeutic implications of PPARgamma in cardiovascular diseases. PPAR Res. 2010; 2010:1–12.

26 Son NH, Park TS, Yamashita H, Yokoyama M, Huggins LA, Okajima K, et al. Cardiomyocyte expression of PPARgamma leads to cardiac dysfunction in mice. J Clin Invest. 2007;117:

2791–2801.
27 Thrailkill KM, Lumpkin CK Jr, Bunn RC, Kemp SF, Fowlkes JL. Is insulin an anabolic agent in bone? Dissecting the diabetic bone for clues. Am J Physiol Endocrinol Metab. 2005;289: E735–E745.
28 Wan Y. PPARγ in bone homeostasis. Trends Endocrinol Metab. 2010;21:722–728.
29 Rzonca SO, Suva LJ, Gaddy D, Montague DC, Lecka-Czernik B. Bone is a target for the antidiabetic compound rosiglitazone. Endocrinology. 2004;145:401–406.
30 Ding J, Woo JT, Nagai K. The effects of retinoic acid on reversing the adipocyte differentiation into an osteoblastic tendency in ST2 cells, a murine bone marrow-derived stromal cell line. Cytotechnology. 2001;36:125–136.
31 Takada I, Yogiashi Y, Kato S. Signaling Crosstalk between PPARγ and BMP2 in Mesenchymal Stem Cells. PPAR Res. 2012;2012:1–7.
32 Goto T, Nagai H, Egawa K, Kim YI, Kato S, Taimatsu A, et al. Farnesyl pyrophosphate regulates adipocyte functions as an endogenous PPARγ agonist. Biochem J. 2011;38:111–119.
33 Koh KK, Han SH, Quon MJ, Yeal Ahn J, Shin EK. Beneficial effects of fenofibrate to improve endothelial dysfunction and raise adiponectin levels in patients with primary hypertriglyceridemia. Diabetes Care. 2005;28:1419–1424.
34 Chou CJ, Haluzik M, Gregory C, Dietz KR, Vinson C, Gavrilova O, et al. WY14,643, a peroxisome proliferator-activated receptor alpha (PPARalpha) agonist, improves hepatic and muscle steatosis and reverses insulin resistance in lipoatrophic A-ZIP/F-1 mice. J Biol Chem. 2002;277:24484–24489.